Electron localization in inhomogeneous Möbius rings

V. M. Fomin,[1] S. Kiravittaya,[1,2] and O. G. Schmidt[1,3]
[1]*Institute for Integrative Nanosciences, IFW-Dresden, Helmholtzstrasse 20, D-01069 Dresden, Germany*
[2]*Department of Electrical and Computer Engineering, Faculty of Engineering, Naresuan University, Phitsanulok 65000, Thailand*
[3]*Material Systems for Nanoelectronics, Chemnitz University of Technology, Reichenhainer Strasse 70, D-09107 Chemnitz, Germany*
(Received 8 July 2012; published 19 November 2012)

The effects of inhomogeneity on the electron states in semiconductor Möbius rings at the microscale are theoretically investigated. Effective electron localization in the untwisted part of an inhomogeneous Möbius ring is caused by a change of the electron quantized kinetic energy. We suggest an experimental method to detect the electron localization by measuring persistent currents in inhomogeneous Möbius rings.

DOI: 10.1103/PhysRevB.86.195421 PACS number(s): 73.22.−f, 73.23.Ra, 04.62.+v

I. INTRODUCTION

Nanostructure fabrication techniques can be exploited to generate nontrivially shaped objects with manmade topological space metrics, which determine the energy spectrum and other physical properties of electrons confined in such nontrivially shaped objects. For instance, spooling a single crystalline $NbSe_3$ ribbon on a selenium droplet by surface tension produces a twist in the ribbon, leading to the formation of a one-sided Möbius strip.[1] The quantum states[2–4] of particles confined in such a topologically nontrivial manifold can be revealed by superconducting properties,[5] persistent currents,[6] the topology-induced Stark shift, spectral splitting, and the quantum decoherence of the pseudospin.[7] The Möbius graphene strip, which is an exotic two-dimensional (2D) electron system with a topologically nontrivial edge, has been proven to be a topological insulator.[8] Energy levels, symmetry, optical transitions, and level splitting in a magnetic field for a homogeneous Möbius ring without thickness have recently been analyzed numerically.[9] Generally, Möbius rings are characterized by an inhomogeneous twist.[10] The degree of *twist localization* is an intrinsic mechanical property of an inhomogeneously twisted Möbius ring. We show in the present paper that it is this *inhomogeneity of the twist* that allows us to quantify the space-dependent metric in Möbius structures by the Aharonov-Bohm quantum-interference effect.

II. GROUND STATE FOR THE SCHRÖDINGER EQUATION IN THE INHOMOGENEOUS MÖBIUS RING: A "DELOCALIZATION-TO-LOCALIZATION" TRANSITION

A Möbius ring with an inhomogeneous twist, spread over *a part* of its circumference, can be formed as shown in Fig. 1. An initial strip with length L_x, width L_y, and thickness L_z shown in Fig. 1(a) is twisted over the length interval L_{x2} [Fig. 1(b)] and then rolled up in a Möbius ring [Fig. 1(c)]. The relative length of the untwisted part of the Möbius ring is $\eta = L_{x1}/L_x$. A finite-element solution of the eigenstate problem for the Schrödinger equation with zero boundary conditions (supported by a variational solution for the ground state of an electron in the inhomogeneous Möbius ring with the space-dependent metric; see Sec. IV) shows that the ground state of an electron confined to the inhomogeneous Möbius ring is expelled from the twisted region already at relatively small values of η. This is illustrated in Fig. 2 (first row) for a set of Möbius rings with $R \equiv L_x/2\pi = 10$ nm, $L_y = 8$ nm, and $L_z = 2$ nm at different values of the untwisted part. At $\eta = 0$, the squared modulus of the ground-state wave function is the same at any cross section normal to the center line of the Möbius ring and reaches its maximal value everywhere on the center line. At $\eta > 0$, the squared modulus of the ground-state wave function on the center line in the untwisted region reaches its maximal value, while its value on the center line in the middle of the twisted region decays towards appreciably low values (for $\eta = 5\%$) and, further, down to 0 (for $\eta = 10\%$ and 20%). An electronic ground-state wave function, which is delocalized and spreads over the whole circumference at $\eta = 0$, becomes *effectively localized in the vicinity of the untwisted region* when increasing the relative length of the untwisted part of the ring.

It is noteworthy that the first excited state changes from delocalized (with maxima of $|\Psi|^2$ that may be arbitrarily positioned on the center line) at $\eta = 0$ to effectively localized in the twisted region at $\eta > 0$ (Fig. 2, second row), the trend of the localization being a slower function of η than that for the ground state. The second and higher excited states remain essentially delocalized at $\eta > 0$ (Fig. 2, third row). In what follows, we focus on the effects due to the effective localization of the ground state.

III. EFFECT OF THE INHOMOGENEOUS TWIST ON THE GROUND-STATE PERSISTENT CURRENT

This "delocalization-to-localization" transition may be detected by measuring the persistent current in the Möbius ring threaded by a magnetic flux Φ through its opening [Fig. 1(c)]. The Aharonov-Bohm oscillations of the persistent current carried by single electron states arise from the periodic dependence of the electron phase on the magnetic flux Φ, leading to a quantum interference pattern that is periodic[11–14] with the period $\Phi_0 = h/e$, where h is Planck's constant and e is the absolute value of the electron charge. The eigenenergies for the lowest states of an electron confined to the Möbius ring are represented as a function of the magnetic flux Φ within one period $0 \leqslant \Phi/\Phi_0 \leqslant 1$ (Fig. 3). Due to the geometric potential,[15] the ground-state energy of an electron in a ring is shifted downwards [green arrow in Fig. 3(a)]. The ground-state energy of an electron in a Möbius ring is shifted upwards [red arrow in Fig. 3(a)] compared to that for a ring made of the

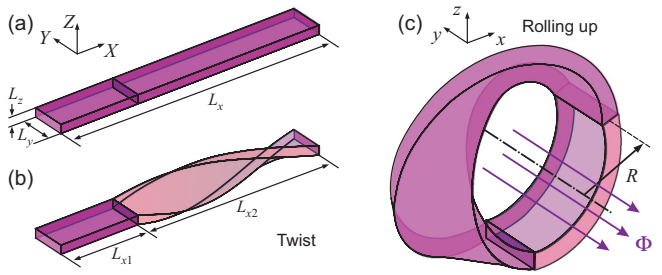

FIG. 1. (Color online) Formation of a Möbius ring with an inhomogeneous twist. The initial strip [with geometric characteristics shown in panel (a)] is twisted only over the length interval L_{x2} (b) and then rolled up in a Möbius ring (c). A characteristic radius of the Möbius ring is $R \equiv L_x/2\pi$. The relative length of the untwisted part of the Möbius ring is $\eta = L_{x1}/L_x$. The electron states are analyzed for a Möbius ring threaded by a magnetic flux Φ through its opening (shown with arrows).

same initial strip [Fig. 3(a)], in qualitative agreement with the behavior revealed for a Möbius ring without thickness.[9] The twist-induced shift of the ground-state energy at zero magnetic field $\Delta E = 22$ meV in a Möbius ring of volume $V = 1.0 \times 10^3$ nm^3 corresponds to an energy density of 2.2×10^{22} eV m^{-3}. The localization of the electron is revealed by a flattening of the ground-state energy as a function of the magnetic flux $E_1(\Phi)$ with increasing ratio

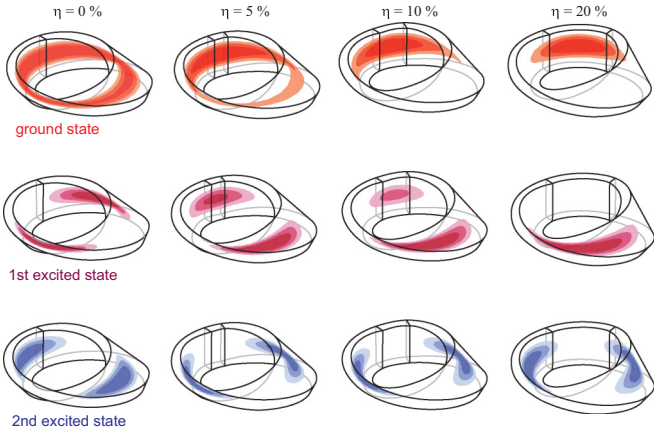

FIG. 2. (Color online) Squared modulus of the wave functions $|\Psi|^2$ of an electron confined to a Möbius ring with an inhomogeneous twist (color code: ground state, red; first excited state, purple; second excited state, blue). Three isosurfaces of the squared modulus of the wave function at 0.7, 0.5, and 0.3 of its maximal value are shown with reducing color intensity. The ground-state wave function is expelled from the twisted region. The magnitude of this expulsion increases when increasing the ratio of the length of the untwisted part of the ring to the whole circumference $\eta = L_{x1}/L_x$. The ground state changes from delocalized at $\eta = 0$ to effectively localized in the vicinity of the untwisted region at $\eta > 0$. The first excited state changes from delocalized at $\eta = 0$ to effectively localized in the twisted region at $\eta > 0$. The second excited state remains essentially delocalized at $\eta > 0$. The localization/delocalization patterns shown for $\eta = 20$ are typical also for larger values $\eta > 20$. The finite-element calculation is performed for the effective mass $m_e = 0.022m_0$, where m_0 is the free-electron mass, and the structural parameters $R = L_x/2\pi = 10$ nm, $L_y = 8$ nm, and $L_z = 2$ nm.

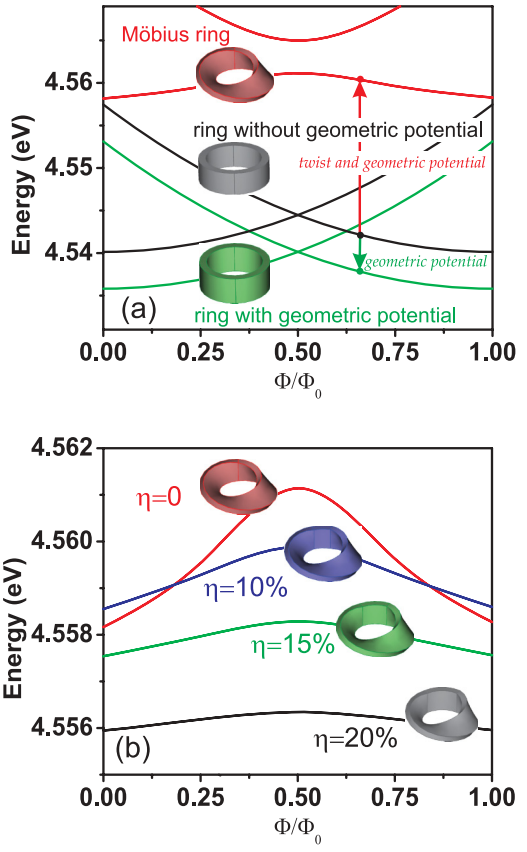

FIG. 3. (Color online) Eigenenergies of the lowest states of an electron in a Möbius ring as a function of the relative magnetic flux. The calculation is performed for $R = L_x/2\pi = 10$ nm, $L_y = 8$ nm, and $L_z = 2$ nm. (a) The ground-state energies of an electron in a ring rolled up from the initial strip shown in Fig. 2(a) are decreased (green arrow down) due to a geometric potential. The ground-state energies of an electron in a Möbius ring are increased (red arrow up) because the increase of the kinetic energy of an electron due to a twist is larger than the energy decrease caused by the geometric potential. (b) When increasing the relative length of the untwisted part η, the expulsion of the electron wave function from the twisted region leads to an overall decrease (except for very small values of η) of the ground-state energy, accompanied by its flattening as a function of the magnetic flux because of an enhanced trend to localization.

$\eta = L_{x1}/L_x$ [Fig. 3(b)]. The ground-state persistent current $I_1(\Phi) = -dE_1(\Phi)/d\Phi$ taken at $\Phi/\Phi_0 = 0.25$ [Fig. 4(a)] shows two distinctly different regions as a function of the ratio η: for lower η, when localization is weak, the current decays by a power law (which, as follows from the fitting of the numerical data, is quadratic), while for higher η it decays exponentially. A boundary between those regions is given by η_{cr}, which quantifies the transition between delocalized and effectively localized states.

The effect of the inhomogeneous twist on the persistent current at low temperatures can be explained as follows. For $\eta = 0$, the electron wave function is uniformly distributed over the whole ring (see the panel $\eta = 0$ in Fig. 2). For $\eta > 0$, the electron wave function tends to be expelled from the twisted region in order to *decrease* the electron energy. This means that the electron state becomes confined to a region (in the vicinity of the untwisted part of the Möbius ring) of smaller length

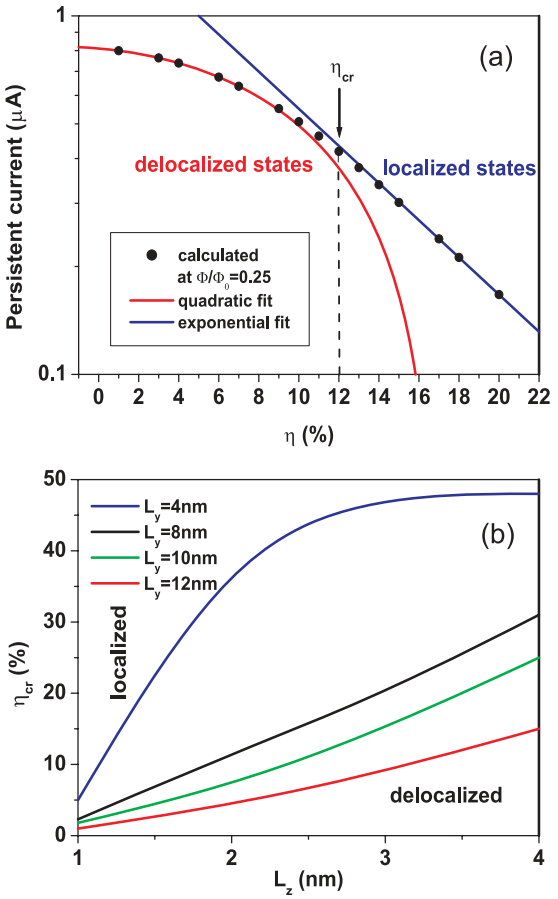

FIG. 4. (Color online) "Delocalization-to-localization" transition in a Möbius ring with an inhomogeneous twist. (a) Persistent current as a function of the relative length of the untwisted part. The values of the persistent current are taken at $\Phi/\Phi_0 = 0.25$. The delocalized states (at lower values of η) reveal a slow (quadratic) decay of the persistent current with increasing η. The effectively localized states (at higher values of η) are characterized by a fast (exponential) decay of the persistent current as a function of η. The value $\eta_{cr} \approx 12$ shown with a dashed line indicates a position of a conventional boundary between the delocalized and effectively localized states. The calculation is performed for $R = L_x/2\pi = 10$ nm, $L_y = 8$ nm, and $L_z = 2$ nm. (b) Phase boundaries for a "delocalized-to-localized" transition obtained from the persistent currents shown in panel (a) plotted as a function of thickness of the Möbius ring. The calculation is performed for $R = L_x/2\pi = 10$ nm.

than the ring's circumference. The kinetic energy quantized due to such a confinement of the circumferential motion ("size-quantized" energy) *increases* as compared to that in a homogeneous Möbius ring. The electron ground state is then a result of an interplay of these counteracting trends, which depends on the relative value of the untwisted part of the Möbius ring. This scenario is confirmed also by the variational solution for the ground state of the Schrödinger equation in the inhomogeneous Möbius ring (see Sec. IV). (i) For small values of η, the energy decrease due to the expulsion of the electron wave function from the relatively large twisted region cannot compensate for the increase of energy due to the size quantization, and the electron wave function is only moderately reduced in the twisted region (see the panel $\eta = 5\%$ in Fig. 2). For the Aharonov-Bohm effect, this implies a small reduction of the persistent current. (ii) With a further increase of η, the twisted region shrinks. Therefore, the energy decrease due to the expulsion of the electron wave function from the twisted region becomes larger than the energy increase due to the confinement of the circumferential motion. As a result, the degree of penetration of the electron wave function into the twisted region quickly decays with increasing η (see the panels $\eta = 10\%$ and 20% in Fig. 2). Consequently, in the presence of an Aharonov-Bohm magnetic flux, the persistent current through the inhomogeneous Möbius ring is progressively hindered with increasing η [Fig. 4(a)]. The boundary values η_{cr} are increasing functions of the thickness L_z in the range from 1 to 4 nm at a given width L_y in the range from 4 to 12 nm [Fig. 4(b)]. For $L_y = 4$ nm, the increase of η_{cr} with thickness is slowed down when the thickness L_z approaches the value of the width (4 nm). For a given thickness L_z, η_{cr} significantly increases upon decreasing the width L_y.

IV. VARIATIONAL SOLUTION FOR THE GROUND STATE OF THE SCHRÖDINGER EQUATION IN THE INHOMOGENEOUS MÖBIUS RING WITH THE SPACE-DEPENDENT METRIC

To find eigenstates of an electron confined to a Möbius ring R, where a twist is spread only over a part of its circumference, we solve the Schrödinger equation

$$\hat{H}\psi = E\psi, \quad \hat{H} = -\frac{\hbar^2}{2m_e}\nabla^2, \quad \nabla^2 = \frac{\partial^2}{\partial x^2} + \frac{\partial^2}{\partial y^2} + \frac{\partial^2}{\partial z^2} \tag{1}$$

in the ring: $(x,y,z) \in R$ with Dirichlet boundary conditions

$$\psi|_{(x,y,z)\in S} = 0 \tag{2}$$

on the surface of the Möbius ring: $(x,y,z) \in S$. The space is Euclidean: the interval is described by the equation $dl^2 = g_{ij}dx_i dx_j$ with a unit Euclidean metric tensor

$$\|g_{ij}\| = \begin{pmatrix} 1 & 0 & 0 \\ 0 & 1 & 0 \\ 0 & 0 & 1 \end{pmatrix}. \tag{3}$$

We recall the procedure of formation of the Möbius ring from a planar strip $P\{(X,Y,Z)\}$ shown in Fig. 1. This procedure generates the transformation of coordinates from the original set $\mathbf{R}(X,Y,Z)$ bound to the initial strip to the final set $\mathbf{r}(x,y,z)$:

$$\begin{aligned} x &= (R - Z)\sin\frac{X}{R}L_{x1}\Theta(L_{x1} - X) + (R - Y\sin\xi - Z\cos\xi) \\ &\quad \times \sin\frac{X}{R}\Theta(X - L_{x1}), \\ y &= Y\Theta(L_{x1} - X) + (Y\cos\xi - Z\sin\xi)\Theta(X - L_{x1}), \\ z &= \left[R - (R - Z)\cos\frac{X}{R}\right]\Theta(L_{x1} - X) \\ &\quad + \left[R - (R - Y\sin\xi - Z\cos\xi)\cos\frac{X}{R}\right]\Theta(X - L_{x1}), \end{aligned} \tag{4}$$

where

$$R = \frac{L_x}{2\pi}, \quad \xi = \kappa(X - L_{x1}), \quad \kappa = \frac{\pi}{L_{x2}}.$$

The coefficient κ is a maximal principal curvature of a twisted strip. The inverse radius $R^{-1} = \kappa_1$ is a maximal principal curvature of a rolled-up strip. Due to the inhomogeneous twist, the twist-related curvature κ can be tuned (to a large extent) independently of the rolling-up-related curvature κ_1. A Heaviside step function $\Theta(X)$ equals 1 if $X > 0$ and 0 otherwise.

We consider further a transformation of the coordinates (4) as *a transformation of space*. It results in the non-Euclidean metric

$$\|g_{ij}\| = \begin{pmatrix} \Phi^2 & 0 & 0 \\ 0 & 1 & 0 \\ 0 & 0 & 1 \end{pmatrix} \Theta(L_{x1} - X) + \begin{pmatrix} \tilde{Y}^2 + \tilde{Z}^2 + \Phi^2 & -\tilde{Z} & \tilde{Y} \\ -\tilde{Z} & 1 & 0 \\ \tilde{Y} & 0 & 1 \end{pmatrix} \Theta(X - L_{x1}), \quad (5)$$

where

$$\Phi = \left(1 - \frac{Z}{R}\right)\Theta(L_{x1} - X) + \left(1 - \frac{Y}{R}\sin\xi - \frac{Z}{R}\cos\xi\right) \times \Theta(X - L_{x1}),$$
$$\tilde{Y} = \kappa Y, \quad \tilde{Z} = \kappa Z.$$

A determinant of the metric tensor (5),

$$g = |g_{ij}| = \Phi^2,$$

represents a change of the elementary volume under the transformation (4): $dxdydz = \sqrt{g}dXdYdZ = \Phi dXdYdZ$. The wave function must undergo a norm-conserving transformation

$$\psi(\mathbf{r}) = \frac{1}{\sqrt{\Phi}}\chi(\mathbf{R}). \quad (6)$$

An inverse of the metric tensor of Eq. (5) is

$$\left\|g_{ij}^{-1}\right\| = \frac{1}{g}\begin{pmatrix} 1 & 0 & 0 \\ 0 & \Phi^2 & 0 \\ 0 & 0 & \Phi^2 \end{pmatrix}\Theta(L_{x1} - X) + \frac{1}{g}\begin{pmatrix} 1 & \tilde{Z} & -\tilde{Y} \\ \tilde{Z} & \tilde{Z}^2 + \Phi^2 & -\tilde{Y}\tilde{Z} \\ -\tilde{Y} & -\tilde{Y}\tilde{Z} & \tilde{Y}^2 + \Phi^2 \end{pmatrix}\Theta(X - L_{x1}). \quad (7)$$

A transformation of the Laplace-Beltrami operator[16]

$$\nabla^2\psi = \frac{1}{\sqrt{g}}\frac{\partial}{\partial X_i}\left[\sqrt{g}(g^{-1})_{ij}\frac{\partial\psi}{\partial X_j}\right],$$

after substitution of Eqs. (5)–(7), leads to the following explicit expression:

$$\nabla^2\psi = \frac{1}{\sqrt{\Phi}}\hat{O}\chi, \quad \hat{O}\chi = \begin{cases} \frac{1}{\Phi^2}\frac{\partial^2\chi}{\partial X^2} + \frac{1}{4R^2\Phi^2}\chi + \frac{\partial^2\chi}{\partial Y^2} + \frac{\partial^2\chi}{\partial Z^2} & \text{for} \quad X < L_{x1}, \\ \frac{1}{\Phi^2}\left(\frac{\partial}{\partial X} + \tilde{Z}\frac{\partial}{\partial Y} - \tilde{Y}\frac{\partial}{\partial Z}\right)^2\chi + \frac{1}{4R^2\Phi^2}\chi + \frac{\partial^2\chi}{\partial Y^2} + \frac{\partial^2\chi}{\partial Z^2} & \text{for} \quad X > L_{x1}. \end{cases}$$

Consequently, the Hamiltonian acquires a complicated form

$$\hat{H} = -\frac{\hbar^2}{2m_e}\left[\alpha^{ij}\frac{\partial^2}{\partial X_i\partial X_j} + \beta^i\frac{\partial}{\partial X_i} + \alpha_0\right],$$
$$\|\alpha^{ij}\| = \begin{pmatrix} \frac{1}{\Phi^2} & 0 & 0 \\ 0 & 1 & 0 \\ 0 & 0 & 1 \end{pmatrix}\Theta(L_{x1} - X) + \begin{pmatrix} \frac{1}{\Phi^2} & \frac{\tilde{Z}}{\Phi^2} & -\frac{\tilde{Y}}{\Phi^2} \\ \frac{\tilde{Z}}{\Phi^2} & \frac{\tilde{Z}^2}{\Phi^2} + 1 & -\frac{\tilde{Y}\tilde{Z}}{\Phi^2} \\ -\frac{\tilde{Y}}{\Phi^2} & -\frac{\tilde{Y}\tilde{Z}}{\Phi^2} & \frac{\tilde{Y}^2}{\Phi^2} + 1 \end{pmatrix}\Theta(X - L_{x1}), \quad (8)$$
$$(\beta^i) = \left(0, -\frac{\kappa\tilde{Y}}{\Phi^2}, -\frac{\kappa\tilde{Z}}{\Phi^2}\right), \quad \alpha_0 = \frac{1}{4R^2\Phi^2}.$$

At the same time, solving the Schrödinger equation $\hat{H}\chi(\mathbf{R}) = E\chi(\mathbf{R})$ is facilitated because the Dirichlet boundary conditions in terms of the coordinates (*X,Y,Z*) are applied on the surface of the planar strip P.

The attractive geometric potential $-\hbar^2/8m_eR^2\Phi^2$ has one and the same form in the regions with and without twist. (Note that here we consider a case of homogeneous rolling up. In systems with *inhomogeneous bending*, the geometric potential gives rise to a trend of localization of the electronic state in the regions with the largest curvature.) If the transverse sizes of the strip are much smaller than its radius R (and hence the length L_x), $L_y \ll R, L_z \ll R$, $\Phi \approx 1$, and we get a geometric potential for a 2D cylinder.[15] The kinetic energy operator in the region with twist contains a coordinate dependence not only via Φ, but also through terms depending on the coordinates $\tilde{Y}$ and $\tilde{Z}$. This leads to a dramatic difference in the behavior of the electron wave function in regions without and with twist in a 3D Möbius ring.

We discuss further a practically relevant case in which the strip has a small width and thickness as compared to its length, $L_y, L_z \ll L_x$, when $\Phi \approx 1$. It is then reasonable to consider the motion along the circumference as slow as compared to the fast motion across the ring and to choose a trial wave function of the form of an adiabatic ansatz,

$$\chi(X,Y,Z) = \Psi(X)\sqrt{\frac{2}{L_y}}\cos\left(\frac{\pi}{L_y}Y\right)\sqrt{\frac{2}{L_z}}\cos\left(\frac{\pi}{L_z}Z\right),$$

which contains the ground-state wave functions describing the electron motion in a strip along the Y and Z directions with the lowest eigenenergies $E_{010}(L_y) = \hbar^2\pi^2/2m_eL_y^2$ and $E_{001}(L_z) = \hbar^2\pi^2/2m_eL_z^2$, correspondingly. This trial wave function obeys the zero boundary conditions for the coordinates Y and Z. Averaging the Hamiltonian (8) with this function, we arrive at the following structure of the electron

energy:

$$E = \langle\chi|\hat{H}|\chi\rangle = E_{100} + E_{YZ} + \Delta E_{\text{roll}} + \Delta E_{\text{twist}} \quad (9)$$

with the kinetic energy of the motion along the circumference

$$E_{100} = -\frac{\hbar^2}{2m_e}\langle\chi|\frac{1}{\Phi^2}\frac{\partial^2}{\partial X^2}|\chi\rangle$$

and the kinetic energy of the motion in the YZ plane confined to a rectangle of sizes $L_y \times L_z$,

$$E_{YZ} = E_{010}(L_y) + E_{001}(L_z),$$

as well as the contributions due to rolling up,

$$\Delta E_{\text{roll}} = -\langle\chi|\frac{\hbar^2}{8m_e R^2\Phi^2}|\chi\rangle,$$

and due to twist,

$$\Delta E_{\text{twist}} = C(L_y/L_z)\frac{\hbar^2\kappa^2}{2m_e}\langle\chi|\frac{1}{\Phi^2}\Theta(X - L_{x1})|\chi\rangle. \quad (10)$$

The coefficient

$$C(L_y/L_z) = \frac{\pi^2 - 6}{12}\left(\frac{L_z^2}{L_y^2} + \frac{L_y^2}{L_z^2}\right) - \frac{1}{2}$$

is a positive function of the ratio of sizes L_y/L_z, reaching its minimal value $\approx$0.14 when the ring has equal width and thickness ($L_y = L_z$). Hence the contribution to the energy due to twist (10) is always *positive*. It can be increased by reducing the spatial extent of the twisted region (via $\kappa = \pi/L_{x2}$). A twist modifies the space metric in such a way that the kinetic energy of an electron in a twisted region of a strip increases as if the electron would have acquired a *smaller effective mass* as compared to the regions of a strip without twist. This makes energetically profitable an expulsion of the electron states from a twisted region to a region without twist. A pattern of the resulting electron wave function is determined by the interplay of the two above-discussed trends: an increase of the kinetic energy due to the geometry-modified metric in a twisted region (ΔE_{twist}) and a rise of the size quantization energy due to confinement in the vicinity of an untwisted region (E_{100}).

The electron energy in an initial strip rolled up into a ring is denoted by the subscript "0" for the Hamiltonian and for the corresponding wave function:

$$E_0 = \langle\chi_0|\hat{H}_0|\chi_0\rangle = E_{010}(L_y) + E_{001}(L_z) + \Delta E_{\text{roll}}, \quad (11)$$

where we take into account the fact that the kinetic energy of the motion along the circumference in the ground state with the azimuthal quantum number equal to 0 vanishes:

$$E_{100} = -\frac{\hbar^2}{2m_e}\langle\chi_0|\frac{\partial^2}{\partial X^2}|\chi_0\rangle = 0.$$

A difference between the electron energy in a Möbius ring with an inhomogeneous twist (8) and that in an initial strip rolled up in a ring (11) is

$$\Delta E = E - E_0 = E_{100} + \Delta E_{\text{twist}}.$$

A relative contribution to the electron energy due to the inhomogeneous twist $\Delta E/E_0$ is estimated to be $\sim 10^{-3}$–10^{-2} for the typical geometric characteristics of Möbius rings. For a given width L_y, the relative contribution $\Delta E/E_0$ increases in Möbius strips with high cross-sectional aspect ratio $L_z/L_y \ll 1$ (or $\gg 1$) as compared to the region of comparable thickness and width: $L_z/L_y \sim 1$. For relatively small thickness L_z, the relative contribution $\Delta E/E_0$ increases when reducing the relative length $\eta = L_{x1}/L_x$ of the untwisted part of the Möbius ring. The maximal values of that contribution range from $\sim 10^{-3}$ for $L_y = 4$ nm to $\sim 10^{-2}$ for $L_y = 12$ nm (see Fig. 5, lower row).

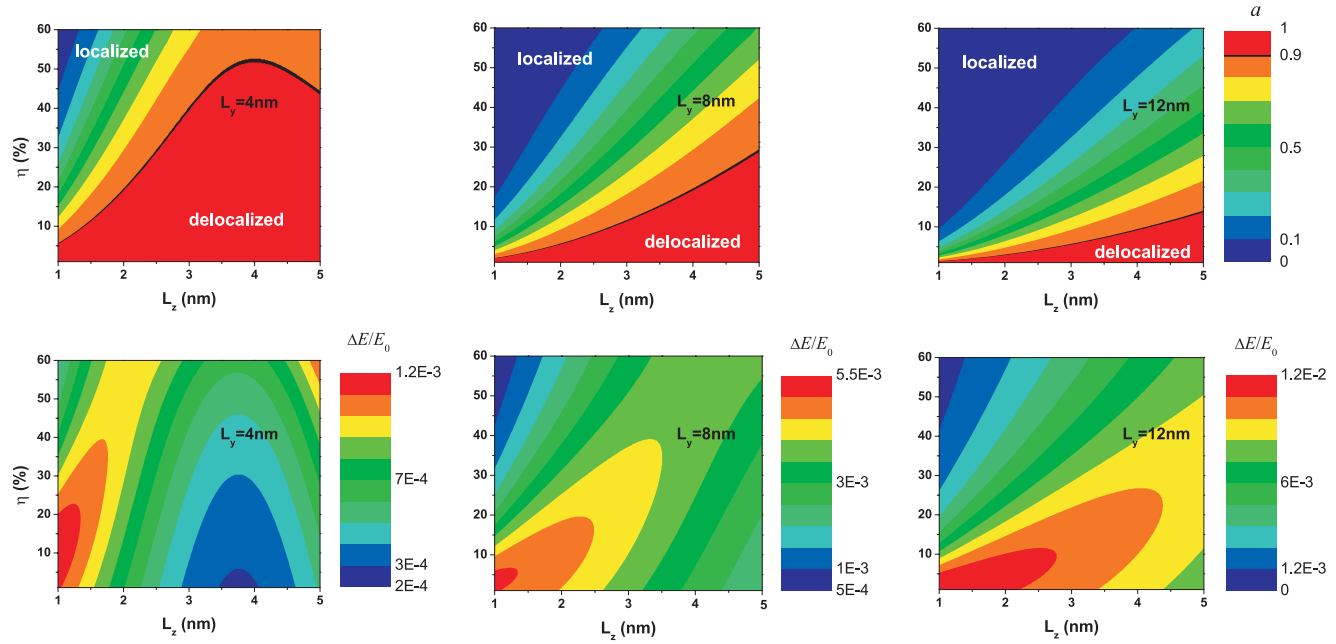

FIG. 5. (Color online) Variational solutions for the amplitude a [Eq. (12)] of the delocalized states (the upper row) and the relative contribution to the electron energy due to twist $\Delta E/E_0$ (the lower row) in a Möbius ring with an inhomogeneous twist. Black lines indicate the level $a = 0.9$, which serves as a conventional localization boundary. The calculation is performed for $R = L_x/2\pi = 10$ nm.

For a thin ring where $L_y \ll R, L_z \ll R$, and hence $\Phi \approx 1$, the average Hamiltonian

$$\langle\chi|\hat{H}|\chi\rangle = E_{100} + E_{010}(L_y) + E_{001}(L_z) + \Delta E_{\text{roll}} + \Delta E_{\text{twist}}$$

with a contribution due to rolling up,

$$\Delta E_{\text{roll}} = -\frac{\hbar^2}{8m_e R^2} \equiv -\frac{\hbar^2\kappa_1^2}{8m_e},$$

contains a trial wave function $\Psi(X)$ in the terms

$$E_{100} = -\frac{\hbar^2}{2m_e}\langle\Psi|\frac{\partial^2}{\partial X^2}|\Psi\rangle$$

$$\text{and} \quad \Delta E_{\text{twist}} = C(L_y/L_z)\frac{\hbar^2\kappa^2}{2m_e}\langle\Psi|\Theta(X - L_{x1})|\Psi\rangle.$$

A trial wave function is selected symmetric with respect to the central point of the untwisted region ($X = L_{x1}/2$),

$$\Psi(X) = \frac{a}{\sqrt{L_x}} + \frac{2b}{\sqrt{3L_{x3}}}\cos^2\left[\frac{\pi}{2L_{x3}}\left(X - \frac{L_{x1}}{2}\right)\right] \times \Theta\left(\left|X - \frac{L_{x1}}{2}\right| - L_{x3}\right), \quad -\frac{L_x}{2} < X - \frac{L_{x1}}{2} < \frac{L_x}{2}. \tag{12}$$

It allows for a continuous tuning between a delocalized state ($a = 1$, $b = 0$) to a localized state ($a = 0$, $b = 1$) with a characteristic localization length L_{x3}. A normalization condition leads to the following link between a and b:

$$a = \sqrt{\left(\frac{4L_{x3}}{3L_x} - 1\right)b^2 + 1} - 2\sqrt{\frac{L_{x3}}{3L_x}}b.$$

The parameters b and L_{x3} are treated as variational parameters. The resulting amplitude a of the delocalized states in a Möbius ring (Fig. 5, upper row) decreases from values close to 1 [which imply delocalized states according to Eq. (12)] to values close to 0 (effectively localized states) when increasing η at a given value of L_z. The level $a = 0.9$ selected as a conventional "delocalization-to-localization" boundary is achieved at higher values of η for a larger thickness L_z at a given width L_y or at a smaller width L_y at a given thickness L_z, when L_z is smaller than the width L_y. When L_z becomes larger than the width L_y, the roles of thickness and width in the above relations interchange, and the level $a = 0.9$ is achieved at lower values of η for a larger thickness L_z at a given width L_y (see the interval $L_z > 4$ nm for $L_y = 4$ nm). This characteristic behavior explains the boundaries for a "delocalized-to-localized" transition obtained in the main text from the persistent current [Fig. 4(b)].

It is worth noting that we consider here a direct, geometry-determined, effect of the inhomogeneous twist on the electronic states in finite-width Möbius rings. As shown in Ref. 4, the eigenstate characteristics are well captured in the absence of hydrodynamic strain using the differential-geometry analysis of Möbius rings.[2] Inhomogeneity of twist of the Möbius ring may lead also to inhomogeneous strain, which is known to control the electronic properties in nonflat heterostructures, e.g., in quantum dots[17] and quantum wires.[18] The strain-induced deformation potential would then give rise to additional electron localization in inhomogeneous Möbius rings.

V. CONCLUSIONS

In summary, symbiosis of the geometric potential and an inhomogeneous twist renders an observation of the topology effect on the electron ground-state energy in microscale Möbius rings into the realm of experimental verification. We predict a "delocalization-to-localization" transition for the electron ground state as the Möbius ring is made more and more inhomogeneous. This transition can be quantified through the Aharonov-Bohm quantum-interference effect on the ground-state persistent current as a function of the magnetic flux threading the Möbius ring. Our theoretical considerations may receive practical relevance in view of the emerging experimental realizations of topologically nontrivial manifolds at the nanoscale, as any pertinent fabrication techniques are likely to generate structural and geometrical inhomogeneities.

ACKNOWLEDGMENTS

We gratefully acknowledge fruitful discussions with P. Cendula, C. Ortix, and J. van den Brink. One of us (S.K.) acknowledges the Naresuan University for support.

[1] S. Tanda, T. Tsuneta, Y. Okajima, K. Inagaki, K. Yamaya, and N. Hatakenaka, Nature (London) **417**, 397 (2002).
[2] J. Gravesen and M. Willatzen, Phys. Rev. A **72**, 032108 (2005).
[3] B. Jensen and R. Dandoloff, Phys. Rev. A **80**, 052109 (2009).
[4] B. Lassen, M. Willatzen, and J. Gravesen, J. Nanoelectron. Optoelectron. **6**, 68 (2011).
[5] M. Hayashi and H. Ebisawa, J. Phys. Soc. Jpn. **70**, 3495 (2001).
[6] K. Yakubo, Y. Avishai, and D. Cohen, Phys. Rev. B **67**, 125319 (2003).
[7] N. Zhao, H. Dong, S. Yang, and C. P. Sun, Phys. Rev. B **79**, 125440 (2009).
[8] Z. L. Guo, Z. R. Gong, H. Dong, and C. P. Sun, Phys. Rev. B **80**, 195310 (2009).
[9] Z. Li and L. R. Ram-Mohan, Phys. Rev. B **85**, 195438 (2012).
[10] E. L. Starostin and G. H. M. Van der Heijden, Nat. Mater. **6**, 563 (2007).
[11] Y. Aharonov and D. Bohm, Phys. Rev. **115**, 485 (1959).
[12] N. Byers and C. N. Yang, Phys. Rev. Lett. **7**, 46 (1961).
[13] F. Bloch, Phys. Rev. B **2**, 109 (1970).
[14] M. Büttiker, Y. Imry, and R. Landauer, Phys. Lett. A **96**, 365 (1983).
[15] R. C. T. da Costa, Phys. Rev. A **23**, 1982 (1981).
[16] L. D. Landau and E. M. Lifshitz, *Field Theory*, 6th ed. (Nauka, Moscow, 1973).
[17] L. He, G. Bester, and A. Zunger, Phys. Rev. B **70**, 235316 (2004).
[18] Z. Ma, T. Holden, Z. M. Wang, G. J. Salamo, L. Malikova, and S. S. Mao, J. Appl. Phys. **101**, 044305 (2007).